Postdoc Fellowships for non-EU researchers

Final Report

Name	Zhenxing Zhang
Selection	2012
Host institution	Ghent University
Supervisor	Prof. Zeger Hens
Period covered by this report	from 01/03/2014 to 28/02/2015
Title	Inorganic Quantum-Dot Light Emitting Diodes, from stack design to micro LEDs

1. Objectives of the Fellowship

The conversion of electricity into light is a key functionality underlying applications such as lighting, optical displays or optical communication. All these examples require a combination of low power consumption, control over the spectrum of the emitted light and, in the case of displays and integrated photonics, miniaturization. Over the past 10 years, various research groups have proposed electrically driven light emitting devices (LEDs) that utilize colloidal QDs as luminescent centers as potentially low power and tunable light sources. The interest in these devices is based on several important advantages colloidal QDs offer over organic dyes or lanthanide-based phosphors as luminescent materials:

- They exhibit spectrally narrow emission providing saturated colors.
- The emission wavelength ranges from the near UV to the mid IR.
- By the growth of inorganic shells, the photostability is strongly enhanced and the photoluminescence quantum yield can be as high is 80-90%.
- They are compatible with various materials and technology platforms.
- Their broad and intense light absorption and short luminescence lifetime enables efficient optical excitation.
- Direct electrical excitation is possible by charge injection or energy transfer.

Similar to organic LEDs, the first generation of QD-LEDs used thin films of small organic molecules and/or semiconductor polymers as contacting layers. Although useful as proof of concept, these devices suffer from significant degradation of the organic components due to both oxidation and electrical damage. As an alternative, QD-LEDs where the light emitting QDs are sandwiched between inorganic electron and hole transport layers have been recently proposed. However, to be of use for display applications or integrated photonics, the conversion efficiency of these devices – currently at 1%1 - needs to be improved, the spectrum of emission wavelengths has to be extended to the near IR and the formation of microLEDs has to be demonstrated.

2. Methodology in a nutshell

The original aim of this project was the development of efficient and wavelength tunable all inorganic QD-LEDs and their miniaturization to form micro LEDs that can be used in display applications and integrated photonics. In practice, this involves:

- ***Optimization of current QD-LED designs*** as proposed in the literature, tackling issues such as nanocrystal charging, poor band alignment and stability under high driving currents.
- ***Extension of the accessible emission wavelengths*** by incorporation of different QDs and the concomitant optimization of the QD-LED design.
- ***Miniaturization towards micro LEDs*** by combining the formation of inorganic QD-LEDs with

standard lithographic techniques.

This project relies on the joint expertise of the UGent research groups PCN (prof. Z. Hens, department of inorganic and physical chemistry, colloidal quantum dots and inorganic LEDs) and PRG (prof. D. Van Thourhout, department of information technology, photonic integration.

At the start of the project, the choice was made to use the recently proposed approach to QD LEDs based on sandwiching colloidal QDs between two insulators after which electroluminescence is induced by applying an alternating, high voltage across this stack. Such an approach can, in principle, be readily combined with SiN-based photonic circuits which may strongly facilitate research results. In this respect, a two-step approach is foreseen where first electroluminescence from QD/SiN stacks is demonstrated and then the problem of integration is dealt with.

3. Results (6-8 pages)

3.1 Quantum dot / SiN stacks for light emission

3.1.1 Device preparation

First we prepared a SiN/QDs/SiN sandwich starting from an ITO layer on glass substrate (provided by Sigma-Aldrich) onto which first a 300nm SiNx layer was deposited using an optimized PECVD process at a temperature of 270^{o}C. A low plasma frequency was chosen to have a low optical loss of the material. Next a close-packed monolayer of colloidal QDs was transferred onto the SiN substrate using spincoating. We used oleate passivated CdSe/CdS core/shell QDs synthesized by a seededgrowth flash approach with a diameter of 9.1 nm and a central emission peak of 622 nm. The quality of the QD layer was examined using atomic force microscopy (AFM). Next a second 200nm SiN layer was subsequently deposited for embedding the QD-layer, using the same PECVD process. In this case a lower temperature (120°C) was used however to minimize impact on the optical quality of the QDs, while still retaining sufficient material quality for the SiN to allow for low-loss photonic devices. A problem that arised using the combination of low temperature and low frequency deposition on a non-flat surface is that the SiN layer started to crack and wrinkle (see **Error! Reference source not found.** on right). This could however be solved by improving the flatness of the QD layer and increasing the growth frequency. Finally Ni/Ag/Au contacts are evaporated on top. A schematic representation of the cross-section of the device is shown in **Error! Reference source not found.**. Next the device was characterized optically and electrically.

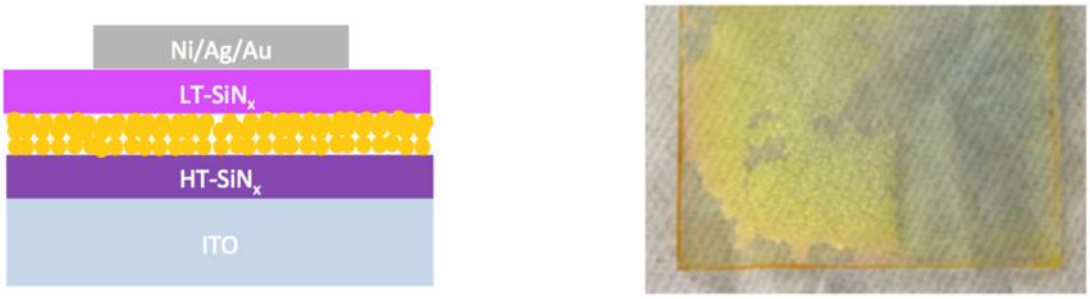

Fig. 1 (left) Schematic representation of the cross-section of the fabricated device. A layer of QDs is sandwiched between two layers of SiNx with a top and bottom electrical contact. (right) Picture of cracked SiNx layer when using a top low temperature and low frequency deposition on QD layer.

3.1.2 Optical properties

The sample is pumped with a blue laser and the photoluminescent intensity versus wavelength is measured using a spectrometer for different QD-layer thicknesses (see **Error! Reference source not found.**). It shows that the peak intensity scales with the thickness of the QD-layer integrated in the device. On the right figure we also notice a shift to the **blue of the central emission wavelength due to self-absorption.**

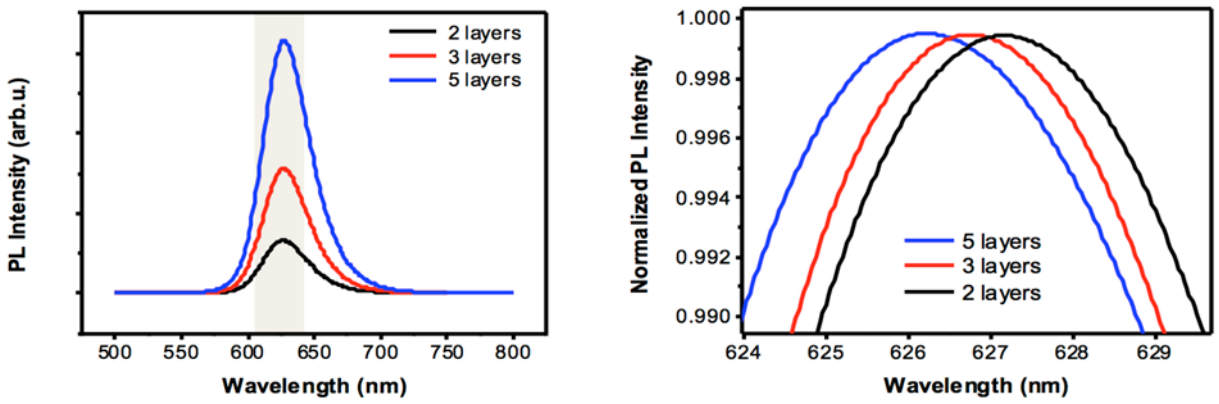

Fig. 2 Photo luminescent intensity versus wavelength for 2, 3 and 5 layers of QDs sandwiched between two SiNx layers

3.1.3. Electrical characterization

The capacitance of the device and a reference sample of SiNx (so without QDs) are measured by applying a low voltage saw-tooth-signal over the sample and a series resistor. We find a capacitance of 4.1 nF and 1.6 nF for the reference sample and the LED-sample respectively. Hence the capacitance of the QD layer is 2.5 nF. Using the formulas of a parallel plate capacitor we obtain that the effective dielectric constant of the QD-layer is equal to 6. From this we can estimate the QD packing *f* using the Maxwell-Garnett mixing rule:

$$\varepsilon_{QD} = \frac{1+\beta f}{1-\beta f}\,\varepsilon_{lig}$$

with $\beta = \frac{\varepsilon_{CdSe/CdS}-\varepsilon_{lig}}{\varepsilon_{CdSe/CdS}+2\varepsilon_{lig}}$ and $\varepsilon_{CdSe/CdS}$ and ε_{lig} the material dielectric constant of the QD and the ligands equal to 10 and 2.2 respectively. We obtain a volume fraction of 67.7%. Next, using the electrical circuit as shown in Fig. 2, a block wave is applied over the LED-device with a specific peak to peak voltage Vpp and frequency. Vout, V(Cs+LED) and V(Cs) are monitored using an oscilloscope (see Fig. 2 on right). From this measurement we can determine the voltage applied over the LED-device (which is in this case 76V) and the voltage applied over a single QD. The latter is calculated by estimating the number of QD layers from the QD-layer thickness and using the impedance of the LED and QD-layer as calculated before. In this specific case we find 7V/QD.

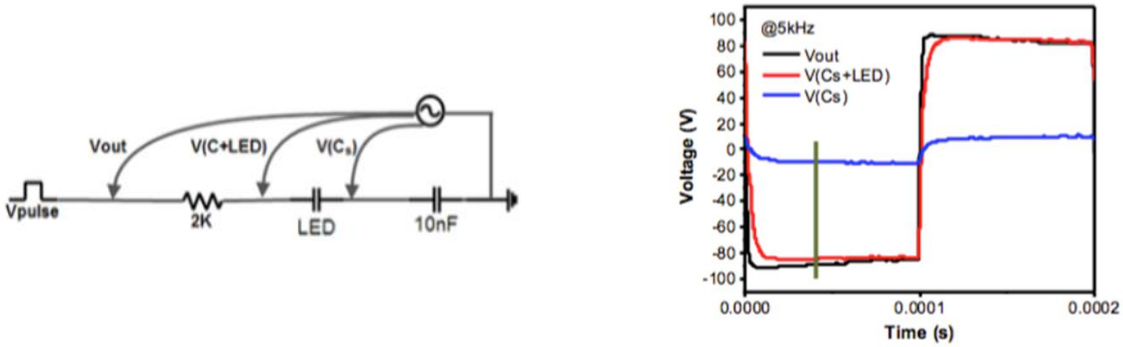

Fig. 2 Schematic representation of the used electrical circuit. By measuring the Voltage as shown in the picture, we can determine V_{LED} and the corresponding V_{QD}. An example of such a measurement is shown on the right.

3.1.4 Electroluminescence

Using the electrical-circuit as described above the electroluminescent performance of the device as a function of applied Vpp and frequency is characterised. The results are shown in **Error! Reference source not found.** and **Error! Reference source not found.** respectively.

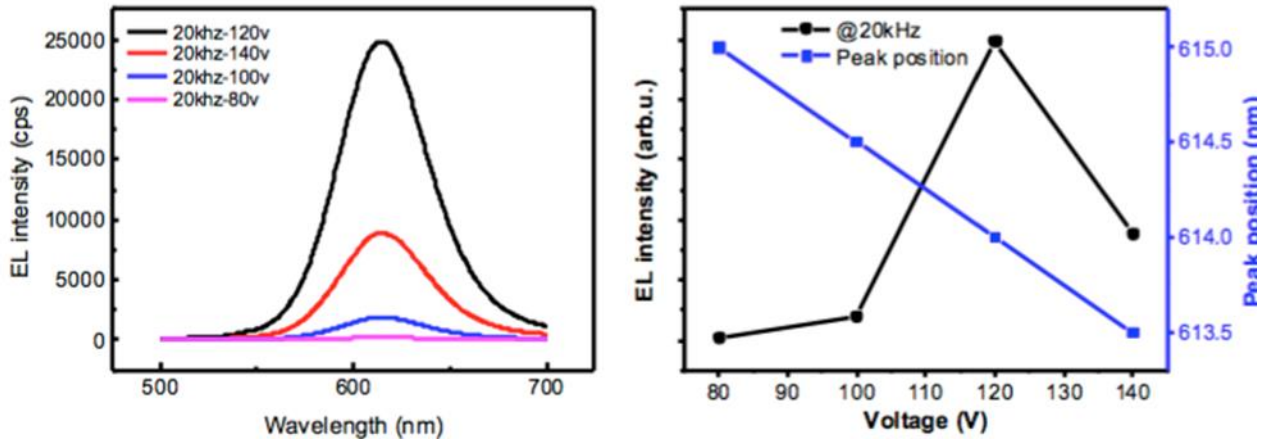

Fig. 4 (left) Electroluminescent intensity as a function of wavelength for various applied voltages and constant frequency of 20kHz. (right) Measured max electroluminescent intensity as a function of the applied voltage.

From **Error! Reference source not found.** we find that the device starts to emit when a signal of 20Hz and Vpp of 160V is applied over the device. The EL intensity increases for increasing voltages with a maximal EL intensity at a Vpp of 240V. When the Vpp is increased even further the intensity decreases again.

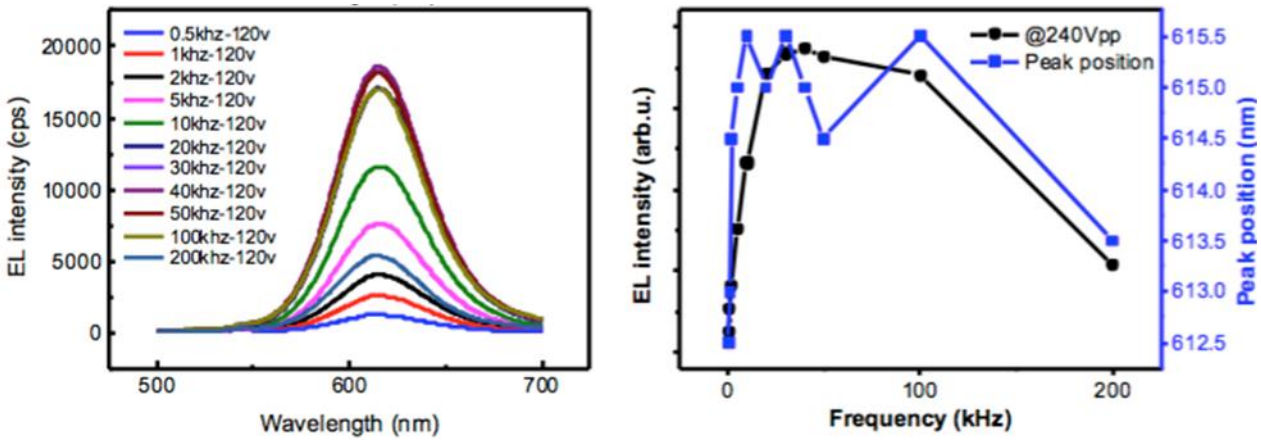

Fig. 5 (left) Electroluminescent intensity as a function of wavelength for various frequencies and constant applied Vpp of 240V. (right) Measured max electroluminescent intensity as a function of the applied frequency.

From **Error! Reference source not found.** we find that at the low frequency range the EL intensity increases with frequency with a maximum at 40kHz. When the frequency is increased further, the charges will not be able to follow the applied alternating signal anymore. Hence the EL intensity will decrease with further increasing frequency. We find a maximum luminance of 16Cd/m^2.

Finally, also lifetime measurements of the device were performed, where the EL intensity for a fixed Vpp and frequency were monitored over a longer period. The decay of the intensity is shown in **Error! Reference source not found.**. We find that the lifetime strongly depends on the applied voltage and

frequency, with decreasing lifetime for increasing voltage and frequency. The degradation of the electrical top contacts can be clearly seen by eye after measurement. An SEM image of such a contact is shown in **Error! Reference source not found.**.

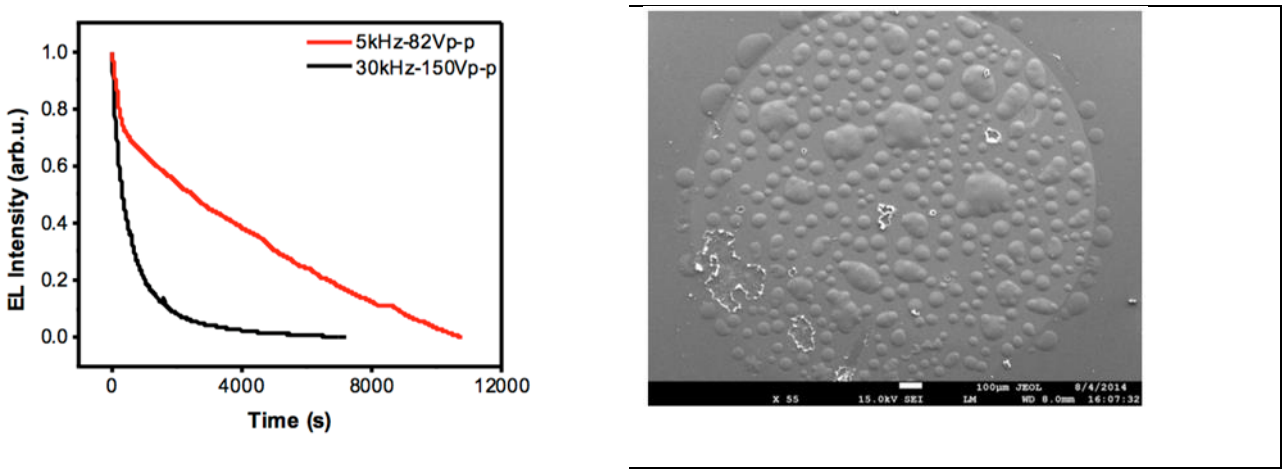

Fig. 6 (left) lifetime measurement of LED device for two different applied Vpp and frequency. The lifetimes are 1.5h and 8min for the red and black curve respectively. (right) SEM image of metal top contact after measurement.

3.2 Quantum dot / SiN stacks as integrated light sources

3.2.1 Simulations and mask design

After the full characterization of our sandaswich structure, we designed a similar structure where the sandwich is etched through to create a waveguide with finite width. As such the QDs and the electrical contacts are integrated in our waveguide to create an integrated electrically pumped light source. As the losses of the guided mode(s) in such a structure strongly depends on the geometry, 2D FDTD simulations were carried out to determine the optimal dimensions of all layers. See Fig. 3 for a schematic representation of the simulated structure. At the sides we have put SU8, as this will be used as insulating layer for separating the two contacts during fabrication (see next section).

Fig. 3 Schematic representation of cross-section of simulated structure.

Using ellipsometry measurements the refractive index of the QD-layer was determined to be equal to 1.89 , we assume no absorption losses coming from the QD-layer. First the thickness of the QD-layer was changed for various SiNx heights. We find the lowest losses of about 500 dB/cm for the thickest QD-layer (210nm) and thick SiNx-layers (>400nm). However, the thicker the waveguide structure becomes the higher the applied voltage over the device needs to be (see **Error! Reference source not found.** on left) to reach the light emitting condition of 2.7V/QD.

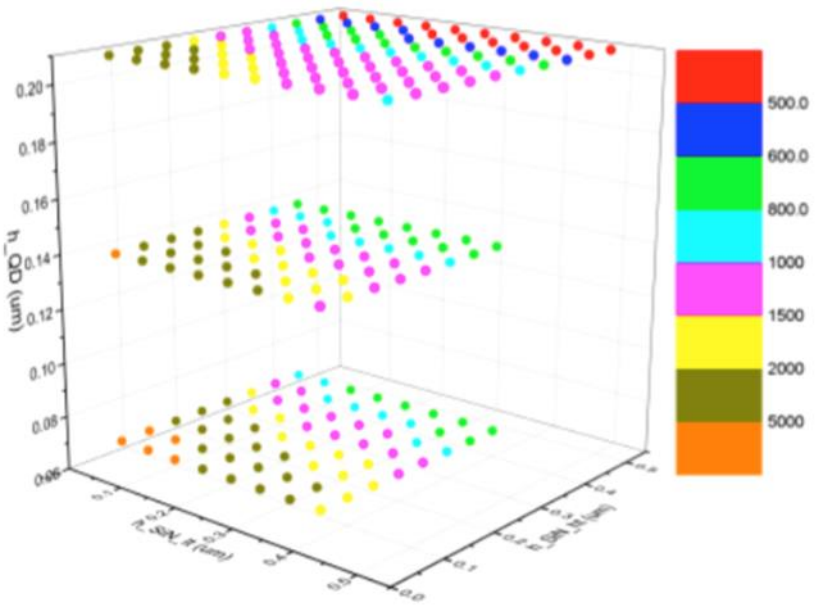

Fig. 4 Simulation results showing the losses in dB/cm for 3 different QD-layer heights and various SiNx top and bottom layer heights.

From simulations we find that the losses vary little when changing the width of the QD-layer. Finally also the thickness of the ITO layer is varied (see Figure 9 on right). We find that the losses increase with increasing ITO thickness. Taking all this into account we choose the optimal dimensions of: SiN-ht = 300 nm, SiN-lt = 200 nm and width QD-layer = 5µm. For the mask design we make a sweep over the area that is covered with QDs. A picture of the GDS-file with all mask-layers are shown in **Error! Reference source not found.** with a zoom of the active area shown in the inset.

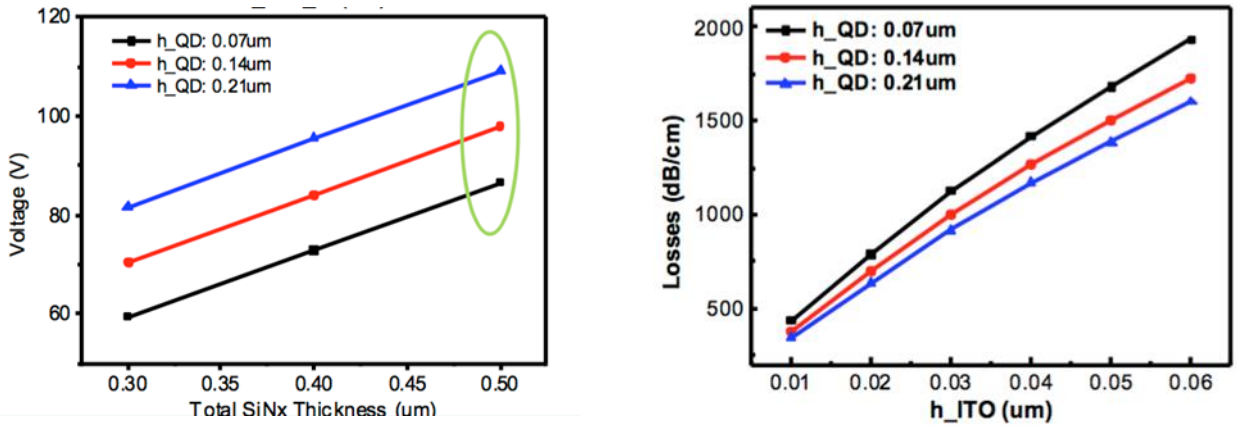

Fig. 9 (left) Voltage that needs to be applied to have light emission versus total SiNx (top+ bottom layer) thickness. (right) losses versus thickness of ITO layer.

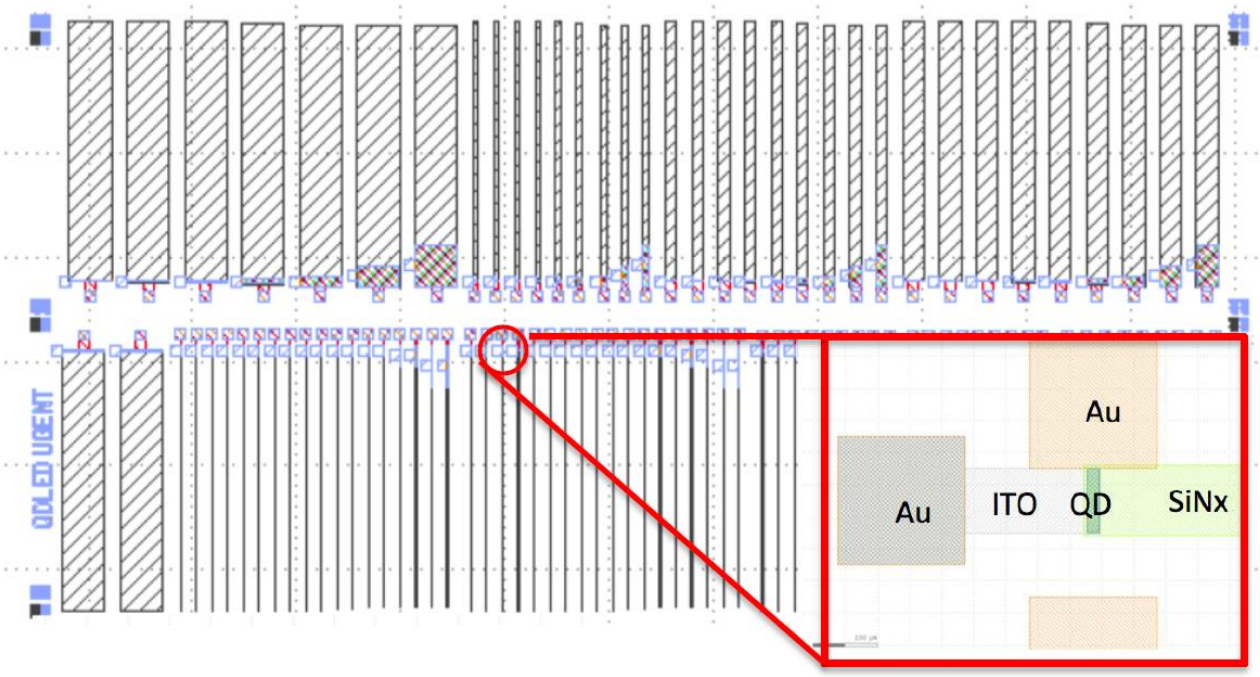

Fig. 10 Mask design. Inset is a zoom in of the active part of the integrated device, containing: area of ITO, and Au contacts and area covered by the QD-layer. Note that the width of the waveguide is chosen to be the same as the width of the QD area.

3.2.2 Fabrication

The fabrication process consists of 5 main steps and with each step corresponds a separate lithography mask.

a. *ITO patterning*: First our mask design for the ITO is patterned using optical lithography and an ICP etching method.

b. *QD deposition*: A first layer of SiNx is deposited. Next a photoresist layer is patterned containing holes for the areas where QDs will stay behind after lift off.

c. *Waveguide formation*: After the second layer of SiNx was deposited the whole structure is patterned using RIE. At this step it is important to not etch too far such that the ITO bottom layer stays intact.

d. *Contact area formation*: Next SU8 (which serves as the insulating layer between the ITO and Au contact) and photoresist are patterned to define the two contact areas.

e. *Metal deposition*: In the last step Au is deposited to define the two metal contacts with which the top and bottom contacts can be contacted. Schematic representations of top and side view of the design are shown below. A Microscopic image of a part of the actual fabricated chip is shown in **Error! Reference source not found.**.

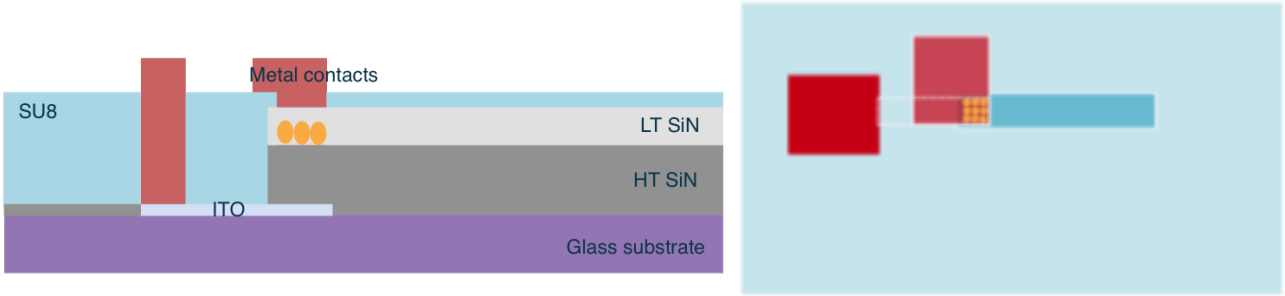

3.2.3 Characterization of fabricated device

To characterize the devices, the chip was cleaved through the waveguides to be able to collect light from the side with a fibre. To ensure proper cleaving the glass substrate was first thinned down. **Error! Reference source not found.** shows the chip with the cleaved facets. As a first step the LEDs were optically pumped with a blue laser from the bottom. Even though red light emission from the QDs could be seen by eye, no light was collected from the cleaved waveguide facet. To explain this additional 3D FDTD-simulations were performed. In these simulations the coupling from a dipole source embedded in a structure as shown in Fig. 3 are calculated. It turned out that the top Au contact acts as a mirror and most of the light is reflected downwards instead of being coupled into the waveguide. Less than 12% of the emitted light is coupled into the waveguide, which is too low to be measured at the facet end. Therefore no additional electrical measurements where performed on the devices.

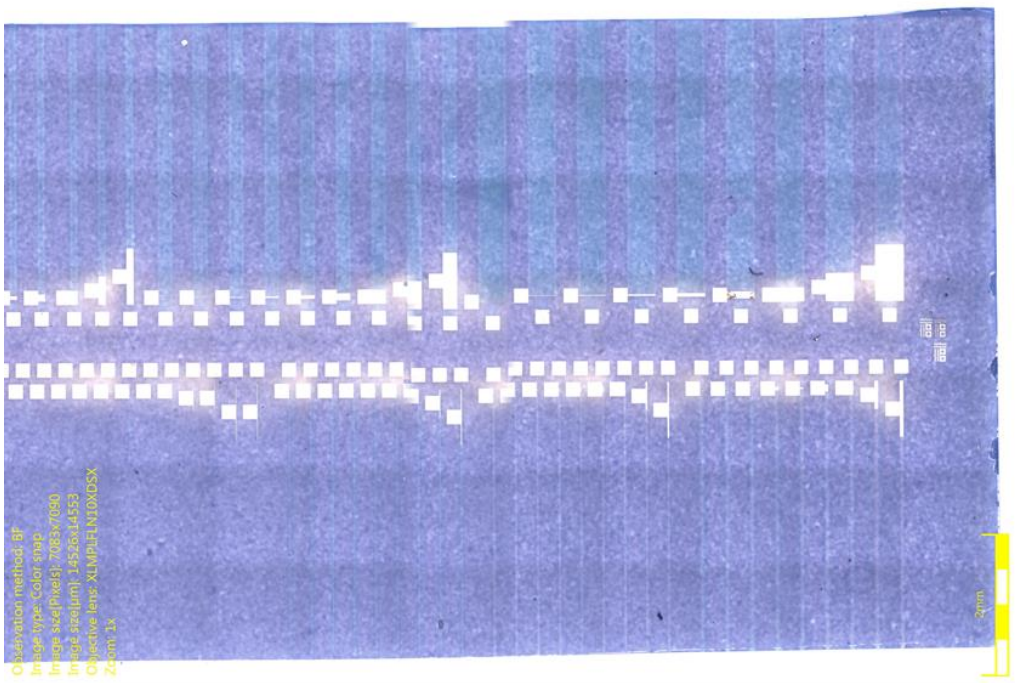

Fig. 11 Microscopic image of the final fabricated chip with light emitting devices.

4. Perspectives for future collaboration between units

The project was a first attempt by UGent-PCN and UGent-PRG to move from optically pumped integrated QD-based light sources to electrically pumped devices as part of their long standing collaboration of QD-based integrated photonics. This proved a daunting task that could not be accomplished within the framework of a 1 year postdoctoral stay, both due to problems with electrical stability of the fabricated devices and the limited coupling efficiency of the light emitted by the QDs in the SiN waveguides.

The exploratory work done by Zhenxing Zhang has been continued at first by a master student, Francis Ryckaert, who looked in particular at improved ways to achieve coupling of light into waveguides. Here, both the option of plasmonic and dielectric enhancement were considered with his work clearly showing that the latter is the preferred way forward. In this respect, new possibilities for QD-based integrated photonics may come from amorphous silicon combined with IR emitting QDs. This offers the high refractive index needed for broadband, high incoupling and it proved possible to embed PbS/CdS QDs within amorphous Si, while retaining their optical properties.

In addition, the challenge of electrically injected, QD-based light sources was picked up by Lukas Elsinger, a PhD student jointly supervised by UGent-PRG and UGent-PCN. Based on the issues encountered by Zhenxing Zhang during his research, this project relies on direct injection of charge carriers through electron and hole transport layers, rather than relying an field-induced carrier injection. Here, first results indicate that a stable, light-emitting junction can be formed.

5. Valorisation/Diffusion (including Publications, Conferences, Seminars, Missions abroad...

Zhenxing Zhang, *AC-driven QD LEDs*, Annual meeting photonics@be, UMONS, October 10, 2014

6. Skills/Added value transferred to home institution abroad

Skills acquired during the stay at UGent involve:

- *Processing and characterization of colloidal quantum dots*. These materials are routinely made at UGent-PCN. Whereas colloidal quantum dot synthesis was not an explicit part of the research project, their processing and optical characterization was. This concerns the formation of QD mono- and multilayers using Langmuir-Blodgett deposition and spincoating, the characterization of these layers by atomic force microscopy and photoluminescence spectroscopy.
- *Electromagnetic field simulations of integrated photonic devices*. A major part of the research project involved the simulation of waveguides doped with QDs and contacted by metal conductors. To explore the optimal configuration – positioning of QDs and contacts, dimensions of the contacts and the QD strip, … - using 2D and 3D FTDT simulations.
- *Clean room fabrication of integrated photonic devices*. An exciting part of the research concerned the actual fabrication of the simulated structures. Here, new skills learned involve the design of masks and the whole series of deposition and lithography steps to eventually fabricate the devices.